

PAPER • OPEN ACCESS

## Occupancy Fluctuation Effect on Metal-Insulator Transition in 3D Hubbard Model within Dynamical Mean-Field Theory Framework

To cite this article: M.G.A. Al Anshori *et al* 2019 *IOP Conf. Ser.: Mater. Sci. Eng.* **515** 012078

View the [article online](#) for updates and enhancements.

# Occupancy Fluctuation Effect on Metal-Insulator Transition in 3D Hubbard Model within Dynamical Mean-Field Theory Framework

M.G.A. Al Anshori, C.N. Rangkuti, M.A. Majidi\*

Department of Physics, Faculty of Mathematics and Natural Sciences, Universitas Indonesia, Kampus UI, Depok 16424, Indonesia

\*Corresponding author's email: aziz.majidi@sci.ui.ac.id

**Abstract.** Dynamical Mean-Field Theory (DMFT) is among the most widely used techniques in computational condensed-matter physics, especially in addressing electron-electron interactions. In this regard, Quantum Monte Carlo may be considered as the most accurate DMFT impurity solver, but it usually requires a high numerical cost. On the contrary, lower numerical-cost technique, such as mean-field theory, often gives inaccurate results due to complete suppression of quantum fluctuations. In this study, we propose a new potentially low numerical-cost impurity solver taking a full account of fluctuation effects. Applying this new algorithm on Hubbard model, we formulate local self-energy that depends on the occupancy fluctuations. These fluctuations act as the semi-classical degree of freedom that needs to be integrated to obtain the averaged fully interacting Green functions. We test our algorithm by addressing temperature dependence of the density of states that reveals metal-insulator transition.

**Keywords:** Occupancy fluctuation effect, metal-insulator transition, 3D Hubbard model, DMFT

## 1. Introduction

Metal-insulator transition (MIT) has been recognized as one among various phenomena signifying that the material belongs to strongly-correlated systems. There are various kinds of MIT, among which there is one that occurs due to strong electron-electron interactions. For this particular phenomenon, the Hubbard model [1] has been commonly used as the basis of explanation. Until now, the model, as well as its variations and extensions, have been used to address many strongly-correlated phenomena resulting from quantum and spatial fluctuations due to electron-electron interactions. Despite intensive research on the Hubbard model, the model is believed to carry still more unexplored features which demand more rigorous techniques to unravel.

Along with that line, numerous numerical approaches based on Green's function method [2] have been developed. In this regard, mean-field theory (MFT) can be considered as the approximation limit in which all forms of fluctuations are fully suppressed. Due to the neglect of fluctuations, one may use MFT results as the benchmark for calculations addressing ground state ( $T = 0$ ) properties of the system. For instance, MFT often gives quite meaningful qualitative results for several physical properties, such as spectral function or density of states (DOS) and magnetic phase. A ground state magnetic phase diagram of the Hubbard model, despite not rigorous, can be constructed through MFT with respect to



Content from this work may be used under the terms of the [Creative Commons Attribution 3.0 licence](https://creativecommons.org/licenses/by/3.0/). Any further distribution of this work must maintain attribution to the author(s) and the title of the work, journal citation and DOI.

variations of the model parameters [3]. However, MFT often fails to correctly capture how physical properties vary with temperature due to the complete absence of fluctuations.

Among existing approaches used to restore the effects of fluctuations, dynamical mean-field theory (DMFT) may have been the most well-recognized approach. It entirely addresses local quantum fluctuations while still neglecting spatial fluctuations [4]. This approach has proved to be quite successful in addressing various temperature-dependent properties of the strongly-correlated system. The key idea is a mapping of the original many-body lattice problem to a many-body local problem embedded inside a self-consistent host, called an impurity problem. This remaining impurity problem can then be solved through a specific algorithm called impurity solver. Various methods of impurity solver have been developed, among them are Quantum Monte Carlo (QMC), exact diagonalization (ED), and numerical renormalization group (NRG). Such methods demand high numerical cost when applied to systems whose size is within the thermodynamic limit. Hence, an alternative method of impurity solver requiring inexpensive computation, yet capable of capturing correct temperature-dependent physical properties of strongly-correlated systems, needs to be developed.

In this paper, we aim to propose a new method of impurity solver for DMFT that offers lower-numerical cost, that works based on the semi-classical treatment of the electron occupancy fluctuations. This new variant of DMFT may be considered as a direct extension of MFT onto which quantum fluctuation of the electron occupancy is added. As a specific case to study, here we choose the Hubbard model at half-filling. This particular model is often used to represent an undoped transition metal oxide material, in which MIT may occur across some transition temperature [5]. We show our results by demonstrating how the density of states evolves with a variation of the model parameters ( $t$  and  $U$ ) and temperature. Also, for comparison, we first perform MIT calculations and address the evolution of DOS and the magnetic phase of the system upon variation of the parameter  $U/t$ .

## 2. The Model

Hubbard model is often applied to transition-metal oxides in which the conduction band is formed by either  $d$  or  $f$  orbital whose wave function is pretty localized in space, resulting in electron hopping effectively occurring only between nearest-neighbour atoms, and that the electron-electron Coulomb interaction works when two electrons stay in the same atomic site. With this picture, we come up with the standard Hubbard model Hamiltonian that reads as shown in Equation 1.

$$H = -t \sum_{\langle i,j \rangle, \sigma} c_{i,\sigma}^\dagger c_{j,\sigma} + U \sum_j n_{j\uparrow} n_{j\downarrow} - \mu \sum_j (n_{j\uparrow} + n_{j\downarrow}), \quad (1)$$

where  $t$  is the hopping integral,  $U$  is the strength of the on-site Coulomb repulsion, and  $\mu$  is the chemical potential of the system. The index  $\langle i, j \rangle$  means that the summation is taken over nearest-neighbour atoms  $i$  and  $j$ . Index  $\sigma$  denotes spin component of the electron.  $c^\dagger$  and  $c$  are creation and destruction operators, respectively, while  $n = c^\dagger c$  is number operator.

Further, as we would like to accommodate possible anti-ferromagnetic (AF) phase, we divide our lattice into two sub-lattices,  $a$  and  $b$ , where every nearest-neighbour atomic sites belong to different sub-lattices. With this picture, we may consider our system as having a crystal structure like that of NaCl, namely that each sub-lattice forms a face-centered cubic (FCC) lattice. Incorporating these two sub-lattices, the Hamiltonian becomes Equation 2-4.

$$H = \underbrace{-t \sum_{i,\sigma} (a_{i,\sigma}^\dagger b_{i,\sigma} + b_{i,\sigma}^\dagger a_{i,\sigma}) + -\mu \sum_{i,\sigma} (n_{ai\sigma} + n_{bi\sigma})}_{\text{non-interacting term}} + U \sum_i (n_{ai\uparrow} n_{ai\downarrow} + n_{bi\uparrow} n_{bi\downarrow}). \quad (2)$$

In the  $U = 0$  limit, the non-interacting term can be Fourier transformed such that

$$H_0 = \sum_{\mathbf{k}, \sigma} \varepsilon_{\mathbf{k}} (a_{\mathbf{k}, \sigma}^\dagger b_{\mathbf{k}, \sigma} + b_{\mathbf{k}, \sigma}^\dagger a_{\mathbf{k}, \sigma}) + -\mu \sum_{\mathbf{k}, \sigma} (n_{a\mathbf{k}\sigma} + n_{b\mathbf{k}\sigma}), \quad (3)$$

where for the given lattice parameter  $c$ ,

$$\varepsilon_{\mathbf{k}} = -2t \left[ \cos\left(\frac{k_x}{2}c\right) + \cos\left(\frac{k_y}{2}c\right) + \cos\left(\frac{k_z}{2}c\right) \right]. \quad (4)$$

### 3. Green Function, Self-Energy, and Density of States

As a common technique used for solving quantum many-body problems, we construct Green function defined in momentum ( $\mathbf{k}$ ) and complex-energy ( $z$ ) space through the Dyson equation as shown in Equation 5.

$$[G(\mathbf{k}, z)] = [z[I] - [H_0(\mathbf{k})] - [\Sigma(\mathbf{k}, z)]]^{-1}. \quad (5)$$

The symbol [...] in Eq. (5) represents a matrix whose row and column indices are determined by the corresponding degrees of freedom of the system, which in this case is the combined index of sub-lattice and spin.  $[H_0(\mathbf{k})]$  is the matrix containing the non-interacting (bare) energy dispersion due to the electron hopping across different sub-lattices, while  $[\Sigma(\mathbf{k}, z)]$  is the matrix representing all the interactions effectively felt by an electron.

As we aim to explore the dynamical properties of the system at finite temperatures, we should work in both Matsubara ( $z = i\omega_n + \mu$ ) and real-frequency or real-energy ( $z = \omega + i0^+$ ) domains. Here  $\omega_n = (2n + 1)\pi k_B T$ , with  $n = 0, 1, 2, \dots$ , is the fermionic Matsubara frequency/energy, while  $\omega$  is the real frequency/energy of the electrons.

From the Green function defined in the real-frequency domain (“retarded” Green function) we can compute the density of states as shown in Equation 6.

$$A(\omega) = -\frac{1}{\pi} \text{Im Tr} \sum_{\mathbf{k}} [G(\mathbf{k}, \omega + i0^+)] \quad (6)$$

and the projected density of states

$$A_\alpha(\omega) = -\frac{1}{\pi} \text{Im} \sum_{\mathbf{k}} G_{\alpha\alpha}(\mathbf{k}, \omega + i0^+). \quad (7)$$

### 4. MIT and Magnetic Phase at the Ground State within MFT

For the Hubbard model, MFT approach essentially replaces the actual two-body interaction terms with the corresponding mean-field version as follows

$$U n_{i\lambda\uparrow} n_{i\lambda\downarrow} \approx U (n_{i\lambda\uparrow} n_{i\lambda\downarrow} + n_{i\lambda\downarrow} n_{i\lambda\uparrow} - n_{i\lambda\uparrow} n_{i\lambda\downarrow}), \quad (8)$$

where  $i$  and  $\lambda$  are, respectively, unit cell and sub-lattice indices. The interpretation is clear, that the up-spin electron interacts with the average number of the down-spin electrons, and vice versa. Thus, the corresponding MFT self-energy matrix contains only diagonal elements that are independent of  $\mathbf{k}$  and  $z$  in the form of

$$\Sigma_\alpha = \langle n_\alpha \rangle U. \quad (9)$$

For self-constant calculation, we set an initial guess for  $\langle n_\alpha \rangle$ , with a constraint that  $\sum_\alpha \langle n_\alpha \rangle$  gives the total electron filling per unit cell, which in this case is 2 for the half-filled system. Along the iteration process, we recompute and then update  $\langle n_\alpha \rangle$  through

$$\langle n_\alpha \rangle = \int A_\alpha(\omega) f(\mu, T, \omega), \quad (10)$$

where  $f(\mu, T, \omega)$  is the Fermi-Dirac distribution function. The self-consistency condition is achieved when the set of calculated  $\langle n_\alpha \rangle$  values are approximately equal, within some tolerance, to those of the input values. Typically, we use a tolerance value about  $1 \times 10^{-5}$ .

### 5. DMFT with Occupancy-Fluctuation Impurity Solver

Calculations beyond MFT have revealed the temperature dependence of MIT [6, 7]. Here, we use the temperature-dependent MIT as a way to demonstrate how our occupancy-fluctuation impurity solver works. The idea behind this new algorithm is based on the semiclassical DMFT implementation for electron-phonon coupling [8] and Hund-like magnetic interaction [9]. We start by expressing the interaction term as shown in Equation 11.

$$\begin{aligned} U \sum_{i\lambda} n_{i\lambda\uparrow} n_{i\lambda\downarrow} &= \frac{U}{2} \sum_{i\lambda} n_{i\lambda\uparrow} n_{i\lambda\downarrow} + n_{i\lambda\downarrow} n_{i\lambda\uparrow} \\ &= \frac{U}{2} \sum_{i\lambda} n_{i\lambda\uparrow} (n_{i\lambda\downarrow} + \delta_{i\lambda\downarrow}) + n_{i\lambda\downarrow} (n_{i\lambda\uparrow} + \delta_{i\lambda\uparrow}), \end{aligned} \quad (11)$$

where  $\delta_{i\lambda\sigma}$  is the fluctuation of the corresponding electron occupancy value  $n_{i\lambda\sigma}$  that we treat as classical quantities varying continuously between  $(-n_{i\lambda\sigma})$  and  $(1 - n_{i\lambda\sigma})$ . In Matsubara-frequency domain, we coarse-grain the Green function over the Brillouin zone as shown in Equation 12.

$$[G(i\omega_n)] = \frac{1}{N} \sum_{\mathbf{k}} [G(\mathbf{k}, i\omega_n)]. \quad (12)$$

The bath Green function is then computed as

$$[\mathcal{G}(i\omega_n)] = [[G(i\omega_n)]^{-1} + [\Sigma(i\omega_n)]]^{-1}. \quad (13)$$

Note that in DMFT, the local quantum fluctuation is preserved by keeping the frequency dependence while suppressing the  $\mathbf{k}$  dependence in the self-energy. Further, we construct the local self-energy matrix whose diagonal elements depend on occupancy fluctuation as

$$\tilde{\Sigma}_{\lambda\sigma} = \frac{U}{2} (n_{\lambda\sigma} + \delta_{\lambda\sigma}). \quad (14)$$

With all these in hand, we then compute the local interacting Green function matrix as

$$[\tilde{G}(i\omega_n, \delta_{a\uparrow}, \delta_{a\downarrow}, \delta_{b\uparrow}, \delta_{b\downarrow})] = [[G(i\omega_n)]^{-1} - [\tilde{\Sigma}]]^{-1}. \quad (15)$$

The effective action that depends on occupancy fluctuation is constructed as

$$\begin{aligned} S_{\text{eff}}(\delta_{a\uparrow}, \delta_{a\downarrow}, \delta_{b\uparrow}, \delta_{b\downarrow}) \\ = - \sum_n \ln \det \left[ [G(i\omega_n)]^{-1} [\tilde{G}(i\omega_n, \delta_{a\uparrow}, \delta_{a\downarrow}, \delta_{b\uparrow}, \delta_{b\downarrow})] \right] e^{i\omega_n 0^+}, \end{aligned} \quad (16)$$

and the corresponding probability function is defined as

$$P(\delta_{a\uparrow}, \delta_{a\downarrow}, \delta_{b\uparrow}, \delta_{b\downarrow}) = \frac{1}{Z} \exp(-S_{\text{eff}}(\delta_{a\uparrow}, \delta_{a\downarrow}, \delta_{b\uparrow}, \delta_{b\downarrow})), \quad (17)$$

with

$$Z = \int d\delta_{a\uparrow} \int d\delta_{a\downarrow} \int d\delta_{b\uparrow} \int d\delta_{b\downarrow} P(\delta_{a\uparrow}, \delta_{a\downarrow}, \delta_{b\uparrow}, \delta_{b\downarrow}) \quad (18)$$

being the partition function.

Now, we average the local interacting Green function matrix over all possible values of occupancy fluctuations

$$[G(i\omega_n)]_{ave} = \int d\delta_{a\uparrow} \int d\delta_{a\downarrow} \int d\delta_{b\uparrow} \int d\delta_{b\downarrow} P(\delta_{a\uparrow}, \delta_{a\downarrow}, \delta_{b\uparrow}, \delta_{b\downarrow}) [\tilde{G}(i\omega_n, \delta_{a\uparrow}, \delta_{a\downarrow}, \delta_{b\uparrow}, \delta_{b\downarrow})]. \quad (19)$$

The lattice self-energy matrix  $[\Sigma(i\omega_n)]$  is then recomputed from the averaged local interacting Green function and bath Green function matrices as

$$[\Sigma(i\omega_n)] = [g(i\omega_n)]^{-1} - [G(i\omega_n)]^{-1}. \quad (20)$$

The Eq. (20) marks the final step of each iteration in the Matsubara-frequency domain. This calculated self-energy matrix is to be inserted back to the Dyson equation (Eq. (5)) for the next Matsubara iteration, and the self-consistency process continues until the self-energy matrix converges.

As we also wish to calculate real-frequency dependent quantities, particularly the DOS, inside the Matsubara-frequency loop we also need to perform the real-frequency iteration. Along with this process, we compute the DOS, the projected DOS, and the chemical potential for which we apply the constraint as given in Eq. (10). The new calculated (updated) chemical potential  $\mu$  is to be used to construct the Matsubara-frequency Green function through Eq. (5) in the next Matsubara-frequency iteration.

## 6. Results and Discussion

### 6.1. MFT Results for the Ground State

As we review in section 3, the phase diagram of ground-state MIT can be obtained by varying the Coulomb repulsion  $U$ , or alternatively the ratio of  $U$  over the hopping integral  $t$ ,  $U/t$ . Figure 1(a) shows the evolution of DOS with variation of  $U$  at  $T = 0$  (ground state), which indicates the transition from metal to insulator occurring as  $U/t$  becomes a finite value, no matter how small. The gap width increases proportionally to  $U$ . In addition, we find that the ground-state magnetic phase is anti-ferromagnetic that also occurs as long as  $U/t$  is finite, as demonstrated in Fig. 1(b), where  $\langle \mathbf{m} \rangle$  is the magnitude of sub-lattice magnetisation or the anti-ferromagnetic order parameter defined as shown in Equation 21.

$$\langle \mathbf{m} \rangle = \langle \mathbf{m}_a \rangle = \langle n_{a\uparrow} \rangle - \langle n_{a\downarrow} \rangle = \langle n_{b\downarrow} \rangle - \langle n_{b\uparrow} \rangle = -\langle \mathbf{m}_b \rangle. \quad (21)$$

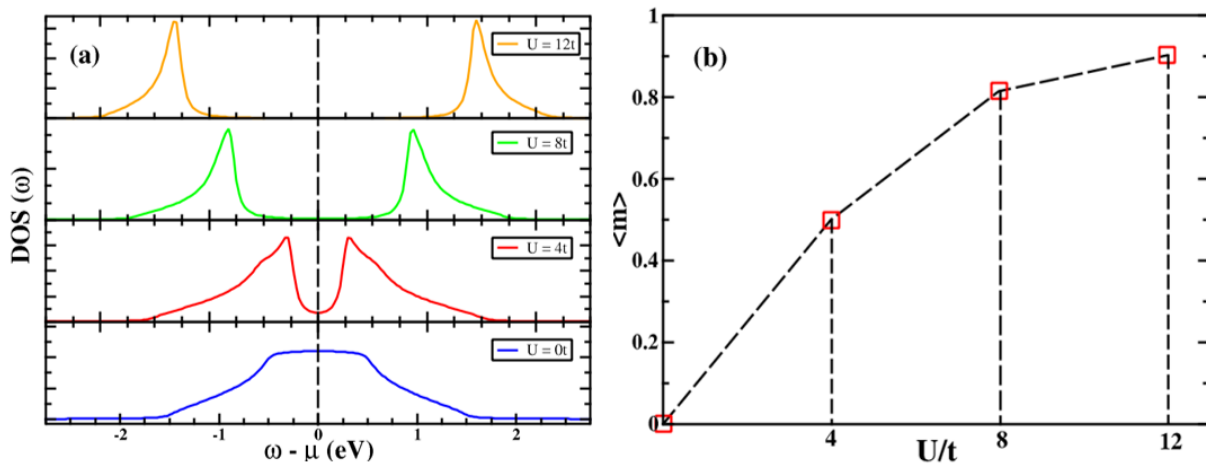


**Figure 1.** MFT results for half-filled system at  $T = 0$ . (a) The evolution of density of states with variation of  $U/t$ . (b) The evolution of sub-lattice magnetization (anti-ferromagnetic order parameter) as a function of  $U/t$ .

Comparing Figs. 1(a) and 1(b), we confirm that the MIT occurs concomitantly with the transition from paramagnetic to ferromagnetic phase. Namely, the non-interacting metallic phase is paramagnetic, while the interacting insulating phase is anti-ferromagnetic.

### 6.2. Occupancy-Fluctuation DMFT Results

For the time being, our occupancy-fluctuation DMFT calculation gives us results which are converged only to paramagnetic phase for all temperatures. However, our results capture the evolution of the gap width as we vary  $U$  as well as  $T$ . Namely, as shown in Fig. 2(a), at fixed  $T$ , as  $U$  becomes larger, the pseudogap broadens and deepens towards a full gap, hence the system becomes more and more insulating. While, as shown in Fig. 2(b), at fixed  $U$ , as  $T$  increases, the already existing full gap tends to diminish becoming a pseudogap and eventually vanish at very high temperatures, hence the system becomes more and more metallic.

Although our results seem to be consistent with the paramagnetic Mott-Hubbard metal-insulator transition experimentally occurring in some real systems, such as  $V_2O_3$  [5], we acknowledge that these results are different from other existing DMFT calculation results for the three-dimensional Hubbard model, where the lowest free energy solution corresponds to anti-ferromagnetic phase. In addition, we also acknowledge that the detailed structure of the DOS at very low temperatures from our results appear to be somewhat different from those of other existing DMFT results, for which their low-temperature solutions correspond to anti-ferromagnetic phase. These issues would be a subject of future development of our algorithm.

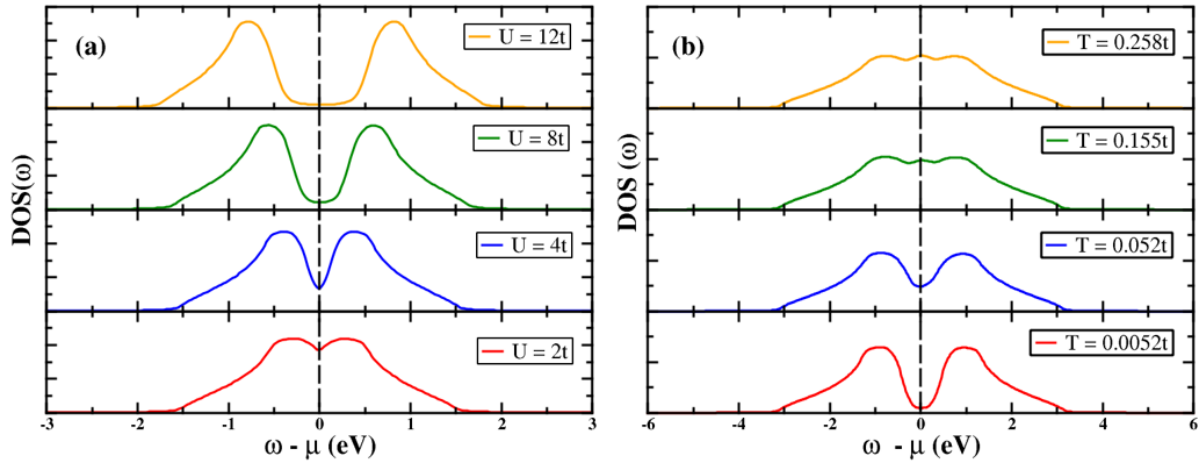


**Figure 2.** Occupancy-fluctuation DMFT results for half-filled system showing paramagnetic MIT. (a) The evolution of the density of states at a fixed low temperature ( $T = 0.0052t$ ) showing paramagnetic Mott-Hubbard MIT, where the MIT occurs as we increase  $U$ . (b) The evolution of the density of states at a fixed value of  $U$  ( $U = 6t$ ), showing that the insulating gap tends to diminish as we increase  $T$ .

Apart from some disagreement between our results and other existing DMFT results, at this point, we would like to comment on the potential superiority of our algorithm compared to the many other DMFT impurity solvers. For instance, within QMC impurity solver, one has to work on the self-consistency process in either Matsubara-frequency or imaginary-time domain. Then, in order to produce the dynamical quantity such as DOS, one has to do a post-processing computation requiring numerical analytic continuation. Such a numerical analytic continuation may be done through Padé approximants [10,11] or maximum entropy method (MEM) [12]. However, those methods are not straightforward that a not-so-careful implementation of those methods may lead to incorrect results. On the contrary, our method directly gives self-consistent results in both Matsubara and real-frequency domains, allowing the user to harvest the dynamical quantities of interest such as DOS directly from the main algorithm. In other words, with this new impurity-solver algorithm a post-processing step for analytic continuation is not necessary to be done.

## 7. Conclusion

We have constructed a potentially low numerical cost DMFT impurity solver for three-dimensional Hubbard model at half-filling. The algorithm is based on the semiclassical DMFT implementation for electron-phonon coupling and Hund-like magnetic interaction, where in this case the electron occupancy fluctuations act as the semi classical quantities. Our results are capable of capturing the dynamics of DOS as functions of Hubbard  $U$  parameter and temperature through the formation and the disappearance of the insulating gap, demonstrating the paramagnetic Mott-Hubbard MIT. Despite some disagreement in the ground state magnetic phase between our results and those of other DMFT impurity solvers, our algorithm offers a potential superiority that the main algorithm can directly produce dynamical quantities such as DOS. We consider any disagreement between our results and those of the more established methods to be a subject for future development of our method.

## References

- [1] R.T.Scalettar 2016 An Introduction to the Hubbard Hamiltonian *Quantum Material: Experiments and Theory* **6** 4
- [2] G.D.Mahan 2000 *Many-Particle Physics 3rd ed* (New York: Springer)
- [3] Y Claveau and B Arnaud and S Di Matteo 2014 Mean-field solution of the Hubbard model: the magnetic phase diagram *European Journal of Physics* **35** 035023
- [4] Georges and G.Kotliar and W. Krauth et al. 1996 Dynamical mean-field theory of strongly correlated fermion systems and the limit of infinite dimensions *Review of Modern Physics* **68** 13
- [5] M. Imada and A. Fujimori and Y. Tokura 1998 Metal-insulator transitions *Review of Modern Physics* **70** 1039
- [6] G. Kotliar and E. Lange and M. J. Rozenberg 2000 Landau theory of the finite temperature Mott transition *Physical Review Letters* **84** 22
- [7] O.N.Ocampo 2017 *Study of the dimer Hubbard Model within Dynamical Mean Field Theory and its application to VO Theses* (Université Paris-Saclay)
- [8] J. Millis, Boris I. Shraiman and R. Muelle 1996 Dynamic Jahn-Teller effect and colossal magnetoresistance in  $\text{La}_{1-x}\text{Sr}_x\text{MnO}_3$  *Physical Review Letters* **77** 1
- [9] N. Furukawa, J. Phys. Soc. Japan **63**, 3214 (1994) and Proc. Conference on Physics of Manganites (1998) (available at <http://xxx.lanl.gov/abs/cond-mat/9812066>).
- [10] C. Titchmarsh 1939 *The Theory of Functions, Fundamental Theories of Physics* (Oxford University Press: London).
- [11] Schött J, Loch I L M, Lundin E, Grånäs O, Eriksson O and Di Marco I 2016 Analytic continuation by averaging Padé approximants *Physical Review B* **93** 1
- [12] Jarrell M and Gubernatis J E 1996 Bayesian inference and the analytic continuation of imaginary-time quantum Monte Carlo data *Physics Reports* **269** 133–95

## Acknowledgements

We are very grateful to Universitas Indonesia for supporting this project with a full-funding through PITTA Research Grant No. 2286/UN2.R3.1/HKP.05.00/2018.